

¹⁴C AMS MEASUREMENTS OF <100 µg SAMPLES WITH A HIGH-CURRENT SYSTEM

KARL F. VON REDEN, ANN P. McNICHOL, ANN PEARSON and ROBERT J. SCHNEIDER

National Ocean Sciences AMS Facility, Woods Hole Oceanographic Institution
Woods Hole Massachusetts 02543 USA

ABSTRACT. The NOSAMS facility at Woods Hole Oceanographic Institution has started to develop and apply techniques for measuring very small samples on a standard Tandemron accelerator mass spectrometry (AMS) system with high-current hemispherical Cs sputter ion sources. Over the past year, results on samples ranging from 7 to 160 µg C showed both the feasibility of such analyses and the present limitations on reducing the size of solid carbon samples. One of the main factors affecting the AMS results is the dependence of a number of the beam optics parameters on the extracted ion beam current. The extracted currents range from 0.5 to 10 µA of ¹²C⁻ for the sample sizes given above. We here discuss the setup of the AMS system and methods for reliable small-sample measurements and give the AMS-related limits to sample size and the measurement uncertainties.

INTRODUCTION

The ongoing trend in AMS toward reducing sample sizes to significantly below 0.1 mg of carbon presents challenges in both sample preparation and AMS data acquisition. The methods of sample preparation (Osborne *et al.* 1994; Vogel, Southon and Nelson 1987) from the stage of original material to that of reduced carbon/catalyst mixture are not greatly affected by the sample size reduction, except that there is a much larger excess of catalyst for small samples than for the “normal” 1-mg sized samples. Making AMS targets out of very small amounts of carbon/catalyst powder is the first challenge. Our automated large-sample target press (Cohen *et al.* 1994) is designed for pellets of 1.5 mm diameter, at least 0.25 mm thick (pressed at 4900 bar). For samples as much as 50 times smaller, the resulting thickness would be too small for sustained AMS sputtering. We therefore manually press the samples into 1-mm-diameter pellets at about the same pressure. The second challenge is the introduction of very small samples into an ion source designed to extract very large currents in normal operation.

In the following sections, we will discuss 1) AMS beam optics in general; 2) our latest results for small-sample measurements; and 3) dilution as an alternative method of dealing with small samples.

AMS BEAM OPTICS

In normal operation with a modern carbon sample (>0.5 mg carbon) we extract at least 35 µA of ¹²C⁻, and detect in excess of 100 particles per second of ¹⁴C (von Reden, Schneider and Cohen 1994). This is an appropriate rate for a reliable setup of the ion beam optics with respect to the transmission of ¹⁴C through the system to the gas ionization detector. For small samples, the extracted ion currents are generally much lower, resulting in low count rates that prevent reproducible detection of changes in the in ¹⁴C/¹²C ratio.

The AMS measurement method compares unknown samples with standards in a sequential fashion and therefore relies on the stability of all system parameters or the exact knowledge of their variation during the measurement period. It has been observed that samples with large differences in size also exhibit large differences in the isotopic fractionation (Brown and Southon 1997). The most likely reason for this effect lies in the ion beam generation itself. Using an ion source modeling program (White 1987) capable of calculating space charge effects for two ion species (here, Cs⁺ and C⁻), we compare two extreme cases for the extraction of ions from a Cs sputter source with hemispherical ionizer. In Figure 1, a section of our ion source is shown with the scale along the beam direction compressed by a factor of 10. The sample is located at the bottom and the ion beam is extracted through

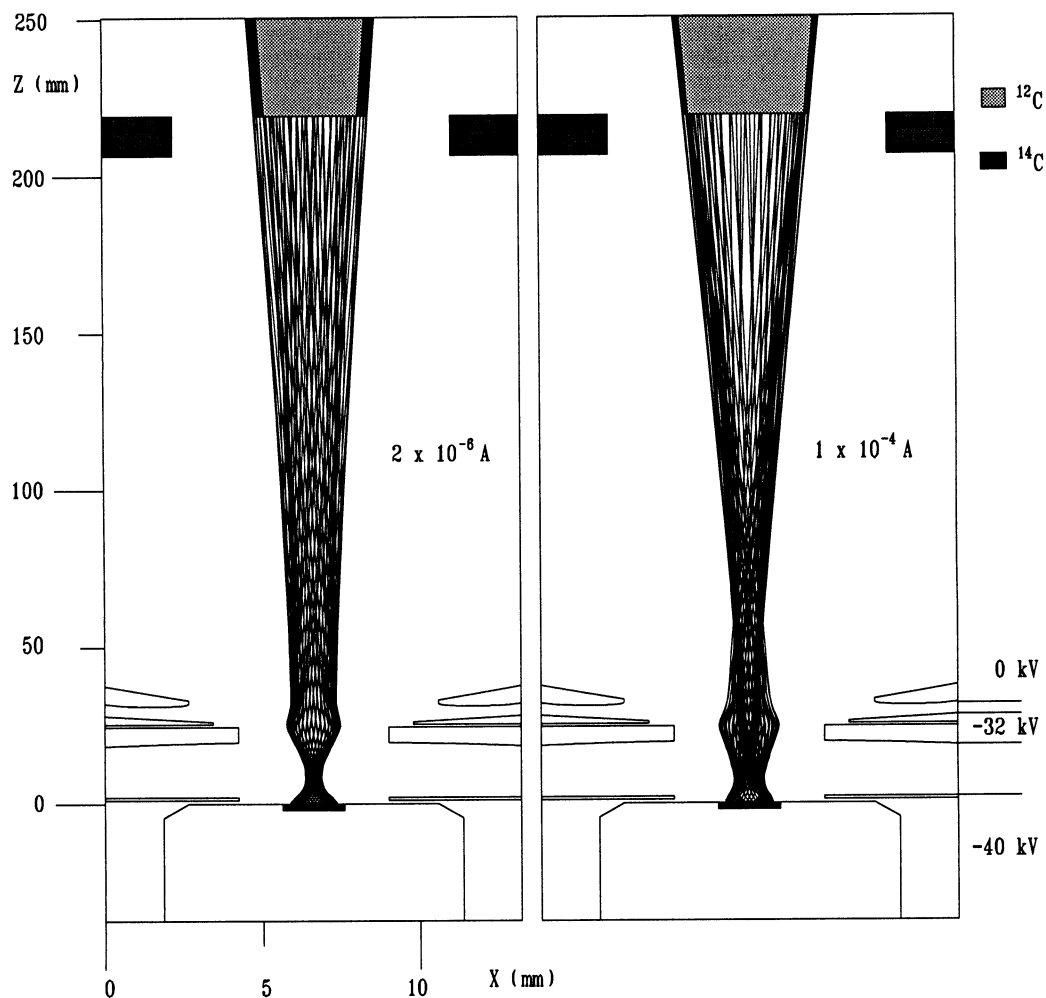


Fig. 1. Model calculations (White 1987) for the extracted negative ion beam from the NOSAMS high-current ion sources. Notice the different scales on the axes. The two cases ($2 \mu\text{A}$ and $100 \mu\text{A}$) represent the small-sample and the “normal” sample limits. Space charge from Cs^+ and C^- is taken into account. The high-current beam displays a larger divergence than would be expected from Coulomb repulsion. There is also a difference in the relative size of the beam diameter between ^{12}C and ^{14}C for the two cases (indicated by the shaded beam envelopes after the einzel lens entrance aperture, $Z = 220 \text{ mm}$). Since the transmission through the AMS system is less than 100%, this implies a dependence of the isotopic fractionation on the extracted beam current.

an aperture in the center of the ionizer in an upward direction. With otherwise identical parameters, only the total extracted negative ion current is changed from $2 \mu\text{A}$ to $100 \mu\text{A}$ in the two cases. These values are close to the observed values for the total negative current for samples containing $<20 \mu\text{g C}$ and $>500 \mu\text{g C}$, respectively. The negative “ion beams” are represented by 40 rays emanating from the 1.5-mm-diameter target with equal fractions of the total beam current at an initial kinetic energy of 2 eV and 45° half angle. The two parts of Figure 1 show the difference in the divergence between the low- and the high-current case. The dominant feature is the size of the first beam waist (ca. 10 mm from the target). Coulomb repulsion leads to a significant increase of the beam diameter at that

point and to the introduction of larger angles in the high-current case. The relative size of the beam envelope diameters for ^{12}C and ^{14}C also differ.

The emittance diagrams (Fig. 2A,B) compare the two beams at a location 38 mm from the target, downstream of the extraction electrode. Again, the introduction of larger divergence angles is visible for the high-current case. The acceptable NOSAMS system beam divergence angle is mainly determined by the terminal stripper canal (1 m long, 12 mm diameter) and has been calculated with RAYTRACE (Kowalski and Enge 1987) to be *ca.* ± 18 mrad at the entrance aperture of the low-energy accelerator tube. Both cases shown here fall well within these limits. However, since none of these calculations take into account realistic beam profiles with halos or tails, it is not possible accurately to predict the dependence of the isotopic fractionation on the beam current. Rather than trying to correct for the dependence of fractionation on sample size, we have adopted the strategy of preparing and comparing standards and unknown samples of equal sizes.

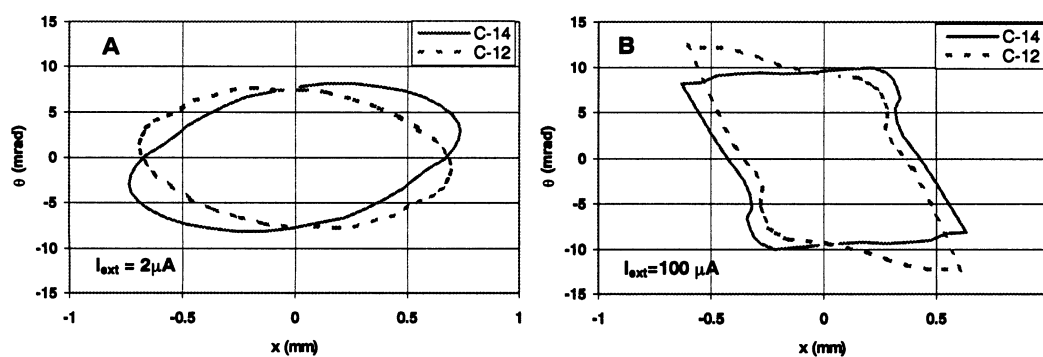


Fig. 2. Emittance diagrams of the extracted ^{12}C and ^{14}C negative ion beams at $Z = 38$ mm (see Fig. 1) for (A) $I_{\text{ext}} = 2 \mu\text{A}$, and (B) $I_{\text{ext}} = 100 \mu\text{A}$. The high-current case displays larger angles and slight convergence (additional waist at $Z = 50$ mm), whereas the low-current beam is nearly parallel at this location.

RESULTS FROM RECENT SMALL-SAMPLE MEASUREMENTS AT NOSAMS

In recent years we have been trying to improve our ability to measure samples with <0.1 mg carbon weight. The advent of preparative capillary gas chromatography (PCGC) has opened up a new domain of research for AMS: ^{14}C analysis of individual organic compounds. For this study, a series of samples ranging from 13 μg to 150 μg C with ^{14}C contents ranging from 0.01 to 1 in units of the fraction of modern carbon (f_{MC}) were analyzed (Fig. 3). Detailed information about the samples and the specific results can be found elsewhere (Eglinton *et al.* 1996; Pearson *et al.* 1998; McNichol, Ertel and Eglinton 1997). In the AMS analysis several observations clarified the present limitations of small-sample AMS at NOSAMS. Fig. 4 shows the extracted beam current as a function of the carbon weight of the sample. Standards, identified by open circles, covered the range from 20 μg to 110 μg . Since the amount of catalyst in all samples was approximately constant, a linear increase of the current with carbon weight was expected, reflecting the areal density of carbon in the exposed surface of the sputter sample. The ^{14}C results for the small-sample standards are compared to the large-sample standard in Figure 5. Several test samples (open squares) were prepared by mixing a known amount of prepared HOxI sample material with a known amount of additional Fe catalyst powder to simulate small sample sizes down to 7 μg carbon weight. These samples exhibit the same AMS performance properties as the others. The measured ^{14}C content drops by up to 10% for the lowest sample weights. The average lifetime of the samples was *ca.* 0.5 h, before sputter depletion pre-

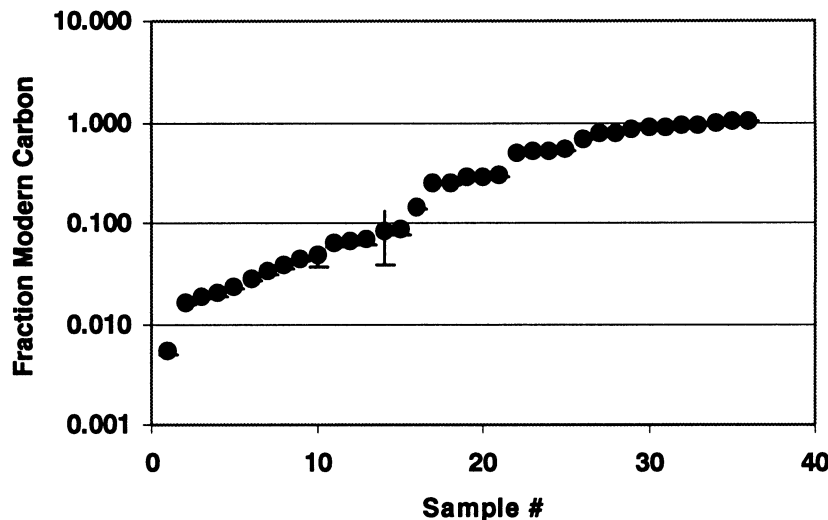


Fig. 3. Range of f_{MC} contents for the small samples analyzed in this paper

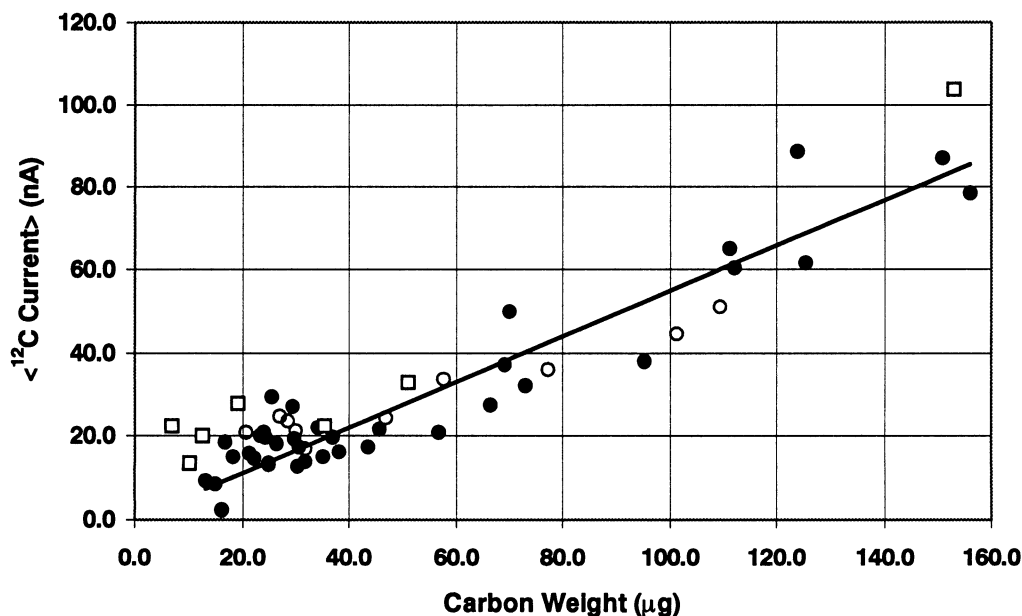


Fig. 4. Analyzed average ^{12}C current as a function of sample carbon weight. Note that the ^{12}C beam current is chopped by a factor of 95 before injection into the accelerator. \circ = standards; \square = test samples generated by mixing known amounts of prepared graphite (HOxI) with additional Fe catalyst powder, before pressing. The carbon/catalyst ratio for all samples ranges from 1% to 10% by weight. Experience at NOSAMS indicates optimum current extraction at C/Fe ratios of 40–50% (Gagnon *et al.* 1997).

vented further AMS analysis. Figure 6 shows the total errors obtained for all samples as a function of the product of carbon weight (W_C) and ^{14}C content (f_{MC}). This method of displaying the uncertainties allows us to state the present limitation for small-sample measurements in terms of the obtainable precision. The measured relative errors very closely follow a $(W_C f_{MC})^{-0.5}$ dependence

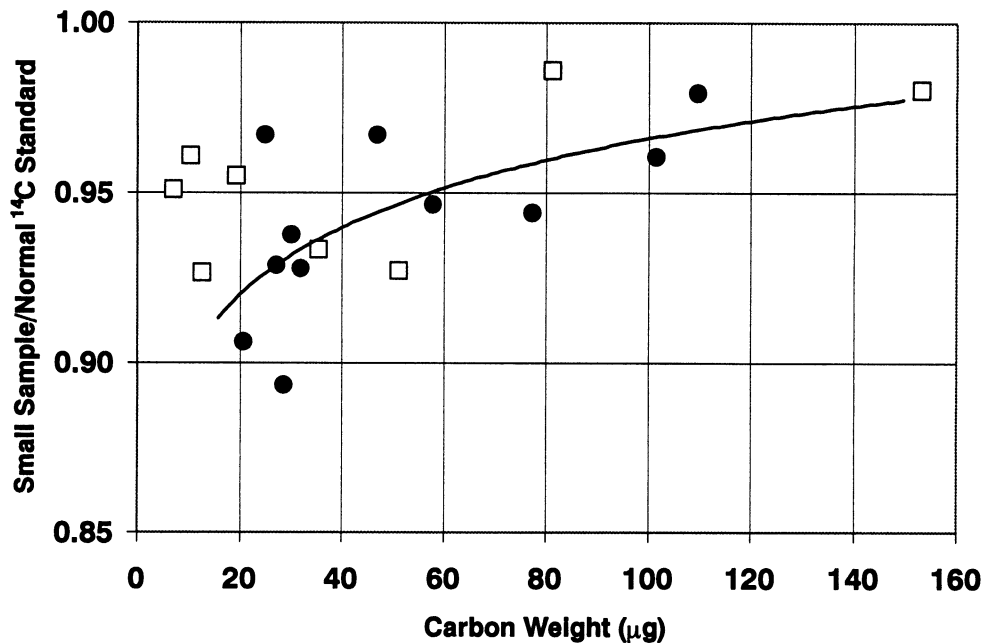


Fig. 5. ¹⁴C results for small-sample standards compared to “normal size” standards. □ = the same test samples as in Fig. 4. Up to 10% fractionation would be introduced by comparing small unknown samples with normal-sized standards.

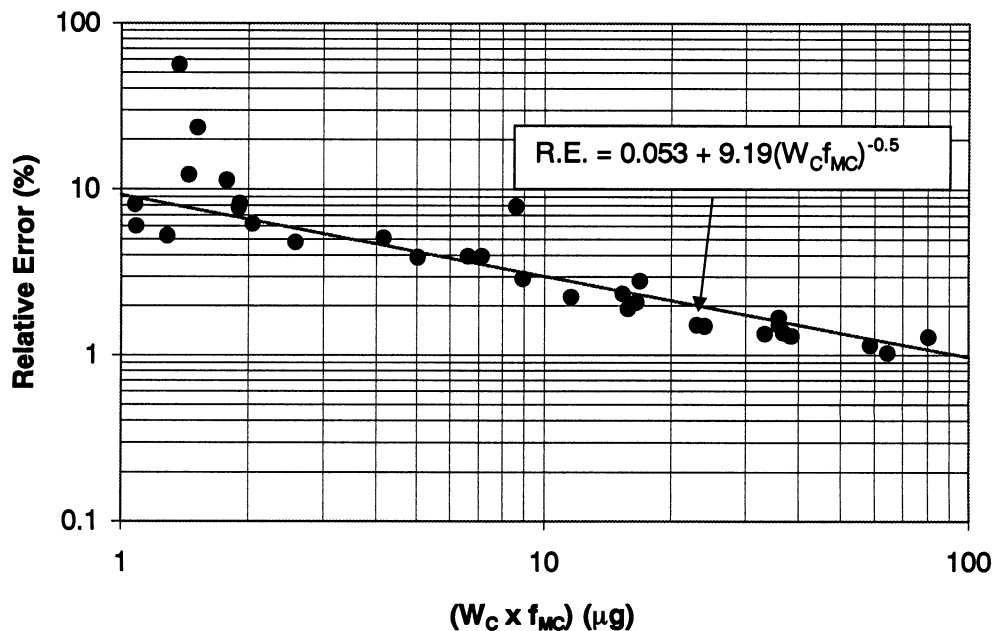


Fig. 6. Total relative error for the samples discussed in this paper, plotted as a function of (carbon weight × f_{MC}). This curve can be used to assess the expected accuracy of small sample analyses at NOSAMS if the approximate age of the material is known. The lower limit for the carbon weight is 15 μg.

down to $W_C f_{MC} = 3 \mu\text{g}$ ($W_C \geq 15 \mu\text{g}$). For the purpose of assessing the feasibility of AMS, this curve can be used to determine the minimum sample size for a sample of an expected ^{14}C content to achieve a desired precision at NOSAMS.

DILUTION

Instead of trying to measure very small samples directly with AMS, chemical dilution in the gas phase of small unknown samples with standard sample gas may be preferable because of better AMS performance. However, taking into account all sources of uncertainty one can establish the conditions under which to choose dilution over direct measurement. Propagation of errors yields:

$$\sigma_{F_s}^2 = r_x^2 \sigma_{F_x}^2 + (1 - r_x)^2 \sigma_{F_d}^2 + 2r_x^2 (F_x - F_d)^2 P^2 + \sigma_{F_{st}}^2,$$

where the F 's designate fractional abundances of ^{14}C for the sample (s), the mixture (x), the diluent (d), and the standard (st), r_x denotes the dilution ratio (mixture weight/sample weight), and P the dilution uncertainty. For undiluted samples $r_x = 1$ and only the first and the last term contribute.

Figure 7 compares the achievable precision for small samples ($\sim 20 \mu\text{g C}$) ranging from 0.063 to 1.0 f_{MC} , using the two methods. We assume for the undiluted measurement: 1) *ca.* $2 \mu\text{A}$ extractable $^{12}\text{C}^-$ ion current with a lifetime of *ca.* 0.5 h of continuous sputtering; 2) the standards measured in comparison yield *ca.* 1.3% precision; 3) background is neglected. For the dilution it is assumed that: 1) the diluent is modern; 2) both the composite sample and the diluent can be measured or are known to 0.5% precision; 3) the uncertainty P of the dilution factor is 1%; 4) background is neglected. The dilution ratios chosen here (4:1–6:1) generate reasonably sized samples (~ 80 – $120 \mu\text{g C}$) making it

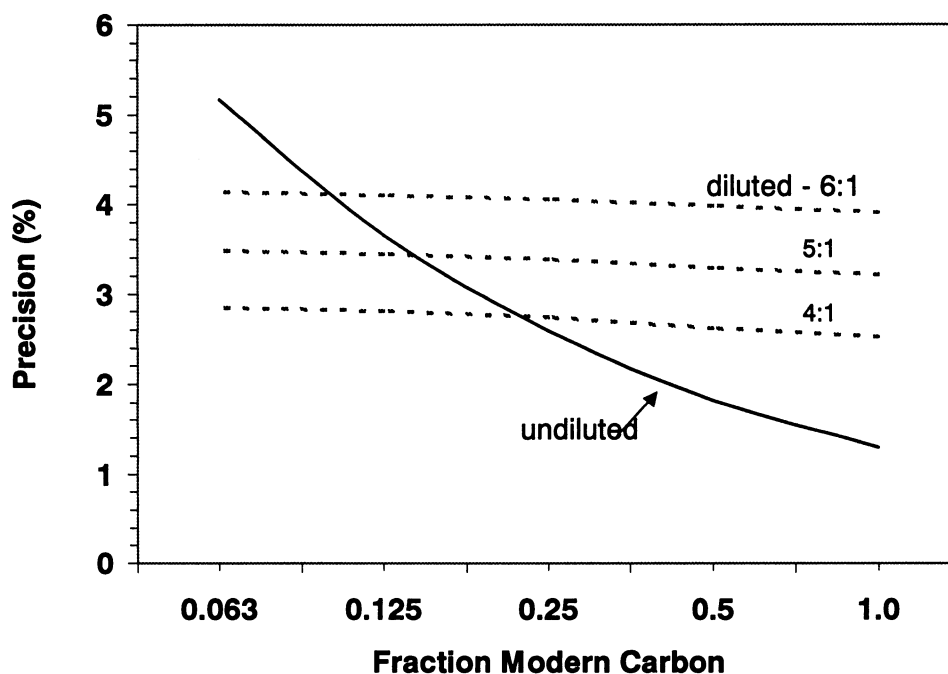


Fig. 7. Expected precision for 20- μg carbon samples as a function of the ^{14}C content, comparing direct measurement with various levels of dilution. See text for the assumptions made in this comparison.

possible to obtain the count rate statistics stated above. A clear result of this comparison is that dilution does not generate any improvement for samples with ^{14}C contents larger than ~25% modern carbon. This crossover may shift somewhat in either direction if backgrounds are significant. Also not taken into account here are measurement uncertainties of the AMS instrumentation for very small currents.

From this discussion it appears that dilution rarely makes sense. However, there are other reasons to consider dilution beside those directly related to AMS. Preparing and handling very small samples is tedious and the risk of losing the sample is considerably higher than for normal-sized samples. If a sample is irreplaceable, dilution is a way to create sufficient sample material for more than one AMS target as a backup.

CONCLUSION

We have established the feasibility of small-sample ^{14}C AMS measurements at the NOSAMS facility for samples as small as 15 µg carbon, depending on their ^{14}C content. From considerations of AMS beam optics and results of small-sample measurements it has become clear that the sample sizes of both unknown samples and standards have to be well matched for accurate AMS analysis. Dilution as a method to overcome the low-current AMS problems presents an improvement only for samples "older" than 25 pMC.

ACKNOWLEDGMENT

This project is supported by the National Science Foundation, under Cooperative Agreement OCE-9301015.

REFERENCES

- Brown, T. A. and Southon, J. R. 1997 Corrections for contamination background in AMS ^{14}C measurements. *Nuclear Instruments and Methods in Physics Research B*123: 208–213.
- Cohen, G. J., Hutton, D. L., Osborne, E. A., von Reden, K. F., Gagnon, A. R., McNichol, A. P. and Jones, G. A. 1994 Automated sample processing at the National Ocean Sciences AMS Facility. *Nuclear Instruments and Methods in Physics Research B*92: 129–133.
- Eglinton, T. I., Aluwihare, L. I., Bauer, J. E., Druffel, E. R. M. and McNichol, A. P. 1996 Gas chromatographic isolation of individual compounds from complex matrices for radiocarbon dating. *Analytical Chemistry* 68(5): 904–912.
- Gagnon, A. R., McNichol, A. P., Donoghue, J. C., Morin, T. J. and Peden, J. C. (ms.) 1997 The National Ocean Sciences AMS (NOSAMS) Sample Preparation Laboratory: Systems and graphite performance analysis. Paper presented at the 16th International ^{14}C Conference, Groningen.
- Kowalski, S. and Enge, H. A. 1987 RAYTRACE [computer program]. MIT, Cambridge, Massachusetts, USA.
- McNichol, A. P., Ertel, J. R., and Eglinton, T. I. (ms.) 1997 Residence time of terrestrial DOM in the ocean: Technique and initial results for radiocarbon content of individual lignin-derived phenols. Paper presented at the 16th International ^{14}C Conference, Groningen.
- Osborne, E. A., McNichol, A. P., Gagnon, A. R., Hutton, D. L. and Jones, G. A. 1994 Internal and external checks in the NOSAMS Sample Preparation Laboratory for target quality and homogeneity. *Nuclear Instruments and Methods in Physics Research B*92: 158–161.
- Pearson, A., McNichol, A. P., Schneider, R. J., von Reden, K. F., and Zheng, Y., Microscale AMS ^{14}C Measurement at NOSAMS. *Radiocarbon*, this issue.
- Vogel, J. S., Southon, J. R. and Nelson, D. E. 1987 Catalyst and binder effects in the use of filamentous graphite for AMS. In Gove, H. E., Litherland, A. E. and Elmore, D., eds., Proceedings of the 4th International Symposium on Accelerator Mass Spectrometry. *Nuclear Instruments and Methods in Physics Research B*29: 50–56.
- von Reden, K. F., Schneider, R. J. and Cohen, G. J. 1994 Performance characteristics of the 3 MV Tandatron AMS system at the National Ocean Sciences AMS Facility. *Nuclear Instruments and Methods in Physics Research B*92:7–11.
- White, N. R. 1987 SORCERY [computer program]. Albion Systems, 21 Friend Court, Wenham, Massachusetts 01984, USA.